PERGAMON International Journal of Multiphase Flow 25 (1999) 501–530

International Journal of Multiphase Flow

Stability in a fully-developed two-dimensional resuspension flow

I. Miskin, L. Elliott *, D.B. Ingham

Department of Applied Mathematical Studies, University of Leeds, Leeds LS2 9JT, UK

Received 9 July 1997; received in revised form 14 September 1998

Abstract

A linear stability analysis examining the stability of a fully-developed, two-dimensional Hagen–Poiseuille resuspension flow is presented. Whilst the analysis includes the non-uniformity of the particle concentration distribution, the inclusion of any concentration fluctuations is ignored. Numerical solutions to the relevant Orr–Sommerfeld equations for temporal disturbance modes are obtained with the aid of ortho-normalization for a variety of different parameters by means of a classical shooting technique. It is found that interfacial instabilities result from long wavelength disturbances even in a small Reynolds number range. The growth rates of disturbances are shown to increase with decreasing initial feed concentration, whilst increasing density stratification is shown to stabilize the resuspension flow. It is also shown that the neglect of fluctuations in the particle concentration severely limits the validity of the stability analysis performed, especially for flows in which the particle concentration in the interfacial region varies rapidly.

Keywords: Particulate resuspension; Stability; Orr–Sommerfeld equation; Interfacial instabilities

1. Introduction

Shear-induced diffusion is the process by which particles within a shear flow migrate permanently across streamlines down gradients in the shear rate and concentration, as a result of interparticle interactions. Previous research has investigated the process of shear-induced diffusion within a number of laminar flows. It has been shown that this process greatly affects the rheology and the flow behaviour of particulate suspensions, i.e. an initially homogeneous flow develops non-uniformities in its concentration distribution, which in turn affects the velocity field within the suspension. An example of this is termed 'viscous resuspension' when

* Corresponding author.

0301-9322/99/$ - see front matter
PII: S0301-9322(98)00061-5

an initially settled bed of negatively buoyant particles, which has a clear fluid layer above, can be resuspended as a result of the shear generated when the clear fluid layer flows. However, in all the situations considered so far, it was assumed that the base flows are steady, see for example Leighton and Acrivos (1986), Schaflinger et al. (1990) and Miskin et al. (1996a). It has then been shown that under certain conditions the interface between the resuspended layer and the clear fluid layer becomes unstable to interfacial waves, which are amplified as they travel downstream in a similar way to those observed in gravity settlers, see for example Herbolzheimer (1983), Shaqfeh and Acrivos (1987), Borhan and Acrivos (1988) and Borhan (1989). Thus, the determination of the stability characteristics for laminar base flows is clearly a matter of interest, especially since under certain flow conditions Schaflinger et al. (1995) observed a considerable discrepancy between the measured and the calculated pressure drop within the channel.

There have been many previous investigations which have examined the stability of two-phase fluid flow phenomena. These flows involving the transport of concentrated slurries have most commonly been examined as 'layered' problems. By this it is implied that the slurry consists of distinct uniform layers, with each layer having different physical properties. Many of these studies have dealt with the stability of convective suspension flows arising in inclined settlers, see for example Acrivos and Herbolzheimer (1979), Schneider (1982), Davis et al. (1983), Shaqfeh and Acrivos (1987), etc. The investigation of Zhang et al. (1992) looked into the stability of a Hagen–Poiseuille suspension flow in a horizontal two-dimensional channel with the effects of surface tension and gravity neglected. In that study, the initial base profiles for the particle concentration, ϕ, and the unperturbed streamwise bulk velocity field, U, were established from viscous resuspension calculations which were performed by Schaflinger et al. (1990). However, since the resulting profiles varied across the channel in a highly nonlinear manner, which would presumably lead to complications in the stability calculations via the solution of the relevant Orr–Sommerfeld equations, Zhang et al. (1992) proposed to consider a mean concentration, $\overline{\overline{\phi}}$, within the resuspended layer. This mean particle concentration was defined as

$$\overline{\overline{\phi}} = \frac{1}{h_t}\int_0^{h_t} \phi(z)\,\mathrm{d}z \tag{1}$$

where z is the non-dimensional distance measured vertically from the bottom surface of the channel and h_t is the value of z at which the interface between the particulate suspension and the clear fluid layer occurs. However, a more appropriate definition than that of the mean particle concentration may be that of a weighted concentration, $\overline{\overline{\phi}}$, namely

$$\overline{\overline{\phi}} = \frac{\int_0^{h_t} \phi(z)u(z)\,\mathrm{d}z}{\int_0^{h_t} u(z)\,\mathrm{d}z} \tag{2}$$

since an experimentalist is likely to maintain a constant particle mass flux as opposed to a constant particle concentration.

This class of problem, i.e. the stability analysis of Couette–Poiseuille type flows in which viscous stratifications exist, has been addressed previously by many researchers, including the theoretical approaches considered by Yih (1967), Yu and Sparrow (1969), Hooper and Boyd

(1983, 1987), Yiantsios and Higgins (1988a,b), etc. and the experimental examination undertaken by Kao and Park (1972). From the aforementioned theoretical studies, it was found that there were essentially two main types of instabilities arising, namely those occurring at small and large Reynolds numbers. Yih (1967) detected instabilities while considering long wavelength disturbances and then demonstrated that viscous stratification alone gave rise to the formation of interfacial waves, even at vanishingly small Reynolds numbers. Hooper and Boyd (1983) noted instabilities when considering short wavelength disturbances, as well as those occurring for long wavelength disturbances, when the stabilizing effects of surface tension were ignored. Yiantsios and Higgins (1988b) extended the work of Yih (1967) and investigated the effects on the 'interfacial mode' of several geometric and physical parameters, such as the thickness ratio, the viscosity ratio and the density ratio of the two fluid system, as well as the surface tension, each of which was allowed to vary independently. In addition, Yiantsios and Higgins (1988a,b) reported that, at sufficiently large Reynolds numbers, the flow may also become unstable to a 'shear mode', which is basically a disturbance of the well-known Tollmien–Schlichting type modified by the presence of an interface.

Zhang et al. (1992) assumed that for their problem, i.e. a Hagen–Poiseuille type suspension flow, that the shear mode similar to that noted by Yiantsios and Higgins (1988a,b) would indeed become unstable at large values of the Reynolds number. Thus, the interfacial mode was the focal point of the study for Zhang et al. (1992) since instabilities due to this mode occurred only at small and moderate values of the Reynolds number, a parameter range of practical significance in the study of viscous resuspension. However, whilst Schaflinger (1994) confirmed the stable range of the interfacial instability determined by Zhang et al. (1992) he also established, contrary to Zhang et al. (1992), that an absolute instability existed and produced some interesting results displaying a complete map of the whole regime of absolute instability with mean concentration as a parameter.

In this paper the problem of the stability of a Hagen–Poiseuille type flow of a particulate suspension is re-addressed, but with a continuously varying particle concentration profile used for the base concentration state as opposed to the averaged profiles considered by Zhang et al. (1992) and Schaflinger (1994). However, it should be stressed that the latter author did not introduce a mean particle concentration on the grounds of the base-state solution, but instead introduced the mean concentration and the resuspension height as independent parameters. This was done, as any reasonable definition for mean concentration seems physically questionable, a result confirmed in the calculation by the fact that the mean concentration, and in turn the viscosity of the suspension, were both extremely sensitive parameters for the stability problem. It should be noted that in this study we follow Zhang et al. (1992), namely we ignore the stabilizing effects of interfacial tension since the suspension and the clear fluid are miscible. A detailed overview of exactly when suspension and clear, overlying fluid can be assumed to be miscible can be found in Joseph and Renardy (1993), where this particular research field commences with the early theory of Korteweg (1901). Whether or not the flow configurations in the suspension and the clear fluid can be treated as representative of miscible fluids is debatable since superimposed miscible fluid can only exist for a finite time, whilst a stratified resuspension can be assumed to be steady. In addition, there is the presence of strong concentration gradients in the resuspension region close to the clear fluid interface which caused Kojima et al. (1984) to introduce the idea of transient interfacial tension.

The resulting Orr–Sommerfeld equation containing derivatives up to second-order in the particle concentration, which vary rapidly in the vicinity of the suspension–clear fluid interface, is solved numerically and the nature of the eigenvalues obtained used to determine the stability behaviour of the flow. Numerical difficulties, such as slow convergence and large CPU times, are likely to abound because of the highly nonlinear nature of the base particle concentration profiles.

2. Basic equations

In Schaflinger et al. (1990) a simple mathematical model, taking into account the effects of sedimentation and the shear-induced diffusion of particles, was used to examine the behaviour of a pressure-driven flow of an initially well-mixed particulate suspension of concentration, ϕ_s, along a plane two-dimensional horizontal channel, see Fig. 1. From this model, the fully-developed particle concentration and bulk velocity fields across the channel have been obtained for a variety of different parameters in Miskin et al. (1996a). It should be noted that the development of the flow from a uniform plug at the entrance of the channel to the fully-developed profile downstream has been addressed in Miskin et al. (1996b). In this section the linear stability of the 'base' resuspension flows similar to those obtained in Schaflinger et al. (1990) will be investigated. Further, in the following analysis the length, velocity and pressure gradient are non-dimensionalised with respect to $2B$, $Q/2B$ and $\mu_1 Q/8B^3$, respectively, where Q is the flux of clear fluid flowing across the channel, $2B$ is the height of the channel and μ_1 is the molecular viscosity of the clear fluid. Since the flow is incompressible, the non-dimensional form of the continuity equation is

$$\frac{\partial u}{\partial x} + \frac{\partial w}{\partial z} = 0 \tag{3}$$

where x and z are the dimensionless lengths along and normal to the channel walls, respectively. It should be noted that $x \in [0,\infty]$ and $z \in [0,1]$, where $z = 0$ and $z = 1$ correspond to the lower and upper surfaces of the horizontal channel, respectively. The dimensionless velocity components in the x and z-directions are denoted by u and w, respectively. On using the continuity Eq. (3), the corresponding two-dimensional Navier–Stokes equations for flow in

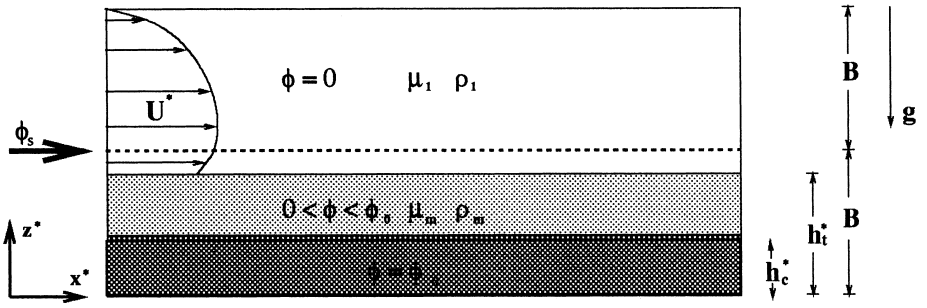

Fig. 1. Schematic diagram of a two-dimensional Hagen–Poiseuille channel flow.

a horizontal channel, see Miskin et al. (1996b), reduce on non-dimensionalization to

$$\rho_r(\phi)\left[\frac{\partial u}{\partial t}+u\frac{\partial u}{\partial x}+w\frac{\partial u}{\partial z}\right]=-\frac{\partial p}{\partial x}+\frac{1}{Re}\left\{\mu_r(\phi)\left(\frac{\partial^2 u}{\partial x^2}+\frac{\partial^2 u}{\partial z^2}\right)+\frac{\partial}{\partial z}\left(\mu_r(\phi)\right)\left(\frac{\partial u}{\partial z}+\frac{\partial w}{\partial x}\right)+2\frac{\partial}{\partial x}\left(\mu_r(\phi)\right)\frac{\partial u}{\partial x}\right\} \tag{4}$$

and

$$\rho_r(\phi)\left[\frac{\partial w}{\partial t}+u\frac{\partial w}{\partial x}+w\frac{\partial w}{\partial z}\right]=-\frac{\partial p}{\partial z}-\frac{9\phi}{2\kappa\, Re}+\frac{1}{Re}\left\{\mu_r(\phi)\left(\frac{\partial^2 w}{\partial x^2}+\frac{\partial^2 w}{\partial z^2}\right)+2\frac{\partial}{\partial z}\left(\mu_r(\phi)\right)\frac{\partial w}{\partial z}+\frac{\partial}{\partial x}\left(\mu_r(\phi)\right)\left(\frac{\partial u}{\partial z}+\frac{\partial w}{\partial x}\right)\right\} \tag{5}$$

where ρ_r and μ_r are the relative density and viscosity, respectively, between the particulate suspension and the clear fluid, and are expressed as

$$\rho_r=\frac{\rho_m}{\rho_1}=\left(1+\eta\phi\right)\quad\text{with}\quad\eta=\frac{\rho_2-\rho_1}{\rho_1}\geq 0 \tag{6}$$

and

$$\mu_r=\frac{\mu_m}{\mu_1}=\left[1+\frac{1.5\phi}{1-\dfrac{\phi}{\phi_o}}\right]^2 \tag{7}$$

respectively, see Zhang and Acrivos (1994), where ϕ is the local particle volume fraction, ϕ_o is the volume fraction of particles in the state of close packing and typically takes the value 0.58, see Leighton and Acrivos (1986) and p is the pressure in excess of the hydrostatic value. It should be noted that the subscripts 1, 2 and m refer to clear fluid, particle and suspension properties, respectively. For this flow the Reynolds number, Re, is defined as

$$Re=\frac{Q}{v_1} \tag{8}$$

where v_1 is the kinematic viscosity of the clear fluid.

The dimensionless form of the unsteady particle concentration equation, which takes into account convective, diffusive and sedimentation effects, see Zhang and Acrivos (1994), can be written as

$$\frac{\partial\phi}{\partial t}+u\frac{\partial\phi}{\partial x}+w\frac{\partial\phi}{\partial z}=\lambda^2\left[\frac{\partial}{\partial x}\left\{\hat{D}_c(\phi)\dot{\gamma}\frac{\partial\phi}{\partial x}+\hat{D}_s(\phi)\frac{\partial\dot{\gamma}}{\partial x}\right\}+\frac{\partial}{\partial z}\left\{\hat{D}_c(\phi)\dot{\gamma}\frac{\partial\phi}{\partial z}+\hat{D}_s(\phi)\frac{\partial\dot{\gamma}}{\partial z}+\frac{\phi f(\phi)}{\kappa}\right\}\right] \tag{9}$$

where the ratio of the particle radii to the height of the channel is given by

$$\lambda = \frac{a}{2B} \tag{10}$$

and κ is the modified Shields number which gives a measure of the ratio between the viscous and buoyancy forces and is given by

$$\kappa = \frac{9}{16}\frac{\mu_1 Q}{B^3 g(\rho_2 - \rho_1)} \tag{11}$$

The non-dimensional shear rate, $\dot{\gamma}$, is expressed as

$$\dot{\gamma} = \left\{ \left(\frac{\partial u}{\partial z} + \frac{\partial w}{\partial x} \right)^2 + 4\left(\frac{\partial u}{\partial x} \right)^2 \right\}^{\frac{1}{2}} \tag{12}$$

In Eq. (9), $f(\phi)$ is the hindered settling function used in this work, see Leighton and Acrivos (1986), and it is expressed as

$$f(\phi) = \frac{1-\phi}{\mu_r} \tag{13}$$

Additionally,

$\hat{D}_c(\phi)$ and $\hat{D}_s(\phi)$ are the shear-induced diffusion coefficients which are given as

$$\hat{D}_c \equiv \frac{D_c}{a^2\dot{\gamma}*} = K_c\phi + K_\mu\phi^2\frac{1}{\mu_r}\frac{d\mu_r}{d\phi}, \quad \hat{D}_s \equiv \frac{D_s}{a^2} = K_c\phi^2 \tag{14}$$

where K_μ and K_c are phenomological constants taken to be 0.65 and 0.43, respectively, see Phillips et al. (1992).

2.1. Boundary conditions

The boundary conditions on the velocity state that fluid cannot penetrate the walls and that there must be no fluid slip at the walls, i.e.

$$u = w = 0 \quad \text{at} \quad z = 0, 1 \tag{15}$$

However, due to the possibility that in the viscinity of the wall the continuum approach for the suspension may fail, Kapoor and Acrivos (1995) introduced a slip condition on the lower boundary which could have an effect on the shear mode instability. The reason for such a modification is that in a distance O(a) from the wall, where a is the particle radius, the discrete nature of the particles influences the flow of the suspension. Since the particles cannot penetrate the wall, their concentration within the O(a) thin wall layer is less than in the bulk, hence the suspension is less viscous. Therefore, the tangential component of the effective bulk velocity, when extrapolated to the wall, will in general differ from the wall boundary. This difference, termed the wall slip velocity, is according to Kapoor and Acrivos (1995) given by $A\mu_r a[(\partial u)/(\partial z)]$, where the numerical value of A varies according to the range of ϕ_s being

considered. In addition, for the suspension, the particle flux must vanish at the walls, i.e.

$$\left(\hat{D}_c(\phi)\dot{\gamma}\frac{\partial\phi}{\partial z}+\hat{D}_s(\phi)\frac{\partial\dot{\gamma}}{\partial z}\right)+\frac{\phi f(\phi)}{\kappa}=0 \quad \text{at} \quad z=0,1 \tag{16}$$

It should be noted that the upper boundary condition [Eq. (16)] reduces to

$$\phi=0 \quad \text{at} \quad z=1 \tag{17}$$

2.2. Base flow

In the event of the flow becoming fully-developed the problem being considered becomes independent of the x-coordinate, as in the problem analysed by Schaflinger et al. (1990), and from the continuity Eq. (3) the velocity component in the z-direction vanishes. Thus, $u\equiv\bar{U}(z)$, $w\equiv 0$ and $\phi\equiv\bar{\phi}(z)$, and from Eq. (5) we can deduce that $(\partial p)/(\partial z)=-[(9\phi)/(2\kappa Re)]$ which, together with the result from Eq. (4) that $[(\partial p)/(\partial x)]$ must either be a function of z or a constant, establishes that $[(\partial p)/(\partial x)]=\text{const.}=-K$, say, where K is the dimensionless pressure gradient. In such circumstances we can recover, via boundary conditions [Eqs. (15)–(17)], the governing momentum and particle concentration equations for the one-dimensional Hagen–Poiseuille base flow, namely,

$$\frac{\mathrm{d}}{\mathrm{d}z}\left(\mu_r(\bar{\phi})\frac{\mathrm{d}\bar{U}}{\mathrm{d}z}\right)=-K \tag{18}$$

and

$$\frac{\mathrm{d}\bar{\phi}}{\mathrm{d}z}=\frac{-(1-\bar{\phi})+\kappa K K_c\bar{\phi}}{\kappa\dfrac{\mathrm{d}\bar{U}}{\mathrm{d}z}\left[(K_\mu-K_c)\dfrac{\mathrm{d}\mu_r}{\mathrm{d}\phi}\bar{\phi}+K_c\mu_r\right]} \tag{19}$$

respectively. The solutions of the system of Eqs. (18) and (19), together with the equations for the conservation of fluid and particles, see Schaflinger et al. (1990), provide the base flow states that will be used in the linear stability analysis which is considered in the next section.

3. Linear stability analysis

Due to the complexity of the problem, in this paper we will neglect perturbations in the particle concentration and perturb the base state for the velocity and pressure as follows:

$$\begin{aligned} u&=\bar{U}(z)+\frac{\partial\hat{\psi}}{\partial z}(x,z,t) \quad , \quad w=-\frac{\partial\hat{\psi}}{\partial x}(x,z,t)\\ p&=\bar{p}(x)+\hat{p}(x,z,t) \quad , \quad \phi=\bar{\phi}(z)\end{aligned} \tag{20}$$

where $\hat{\psi}$ and $\hat{p}$ are normal mode disturbances which take the form

$$\hat{\psi} = \psi(z)\exp\left[\mathrm{i}(\alpha x - \omega t)\right] \quad , \quad \hat{p} = h(z)\exp\left[\mathrm{i}(\alpha x - \omega t)\right] \tag{21}$$

respectively. Additionally, α and ω are the complex wavenumber and frequency, respectively.

By substituting Eqs. (20) and (21) into Eqs. (4) and (5), linearizing and eliminating h, we obtain

$$\begin{aligned}&\mathrm{i}\rho_{\mathrm{r}}\left\{\left(\alpha\bar{U}-\omega\right)\left(\psi''-\alpha^2\psi\right)-\alpha\bar{U}''\psi\right\}+\mathrm{i}\rho_{\mathrm{r}}'\left[\left(\alpha\bar{U}-\omega\right)\psi'-\alpha\bar{U}'\psi\right]\\&\quad=\frac{1}{Re}\left\{\mu_{\mathrm{r}}\left(\psi^{\mathrm{iv}}-2\alpha^2\psi''+\alpha^4\psi\right)+2\mu_{\mathrm{r}}'\left(\psi'''-\alpha^2\psi'\right)+\mu_{\mathrm{r}}''\left(\psi''+\alpha^2\psi\right)\right\}\end{aligned} \tag{22}$$

which is the modified Orr–Sommerfeld equation taking into account the variation of density and viscosity and where $'$ denotes differentiation with respect to z.

3.1. Boundary conditions

The boundary conditions for the fluid require the tangential and normal components of the fluid velocity to be continuous at the boundaries, namely the fluid not to penetrate or slip at the boundaries. Thus, for the perturbed flow, we require

$$\psi = \psi' = 0 \quad \text{at} \quad z = 0, 1 \tag{23}$$

It should be noted that when the flow is perturbed the position at which the suspension–clear fluid interface arises changes from $z = h_{\mathrm{t}}$ to $z = h_{\mathrm{t}} + \eta(x,t)$. For the base flow, the normal and tangential shear stresses and velocities vary continuously across the interface. This should also be true in the perturbed case when the interface occurs at $z = h_{\mathrm{t}} + \eta$, which requires the derivation of alternative continuity relations for the normal and tangential shear stresses and velocities. These conditions have been derived previously by Yih (1967). In the current analysis, as a result of the utilization of a continuous base particle concentration profile, the continuity of normal and tangential shear stresses and velocities simply requires ψ and its derivatives to be continuous across the suspension–clear fluid interface, i.e.

$$\psi_{\mathrm{A}} - \psi_{\mathrm{B}} = \psi'_{\mathrm{A}} - \psi'_{\mathrm{B}} = \psi''_{\mathrm{A}} - \psi''_{\mathrm{B}} = \psi'''_{\mathrm{A}} - \psi'''_{\mathrm{B}} = 0 \quad \text{at} \quad z = h_{\mathrm{t}} + \hat{\eta} \tag{24}$$

where the subscripts A and B refer to the properties of the clear fluid and the suspension, respectively. The matching condition Eq. (24), together with Eq. (22) and the boundary condition [Eq. (23)], constitute a classical eigenvalue problem in that for each set of parameters there exists at least one discrete complex eigenvalue, namely, the complex wavenumber α, or the complex frequency ω, respectively. In the next section we discuss a numerical procedure used to solve such Orr–Sommerfeld eigenvalue problems.

4. Solution technique

In this paper we use a shooting method with an ortho-normalization procedure which involves the integration of the governing stability Eq. (22) within the clear fluid and the suspension layers from the upper and lower boundaries to the interface $z = h_{\mathrm{t}}$, respectively, for

a given set of parameters ϕ_s, κ, η and Re and an initial guess for the eigenvalue ω (or α). It should be noted that in this study we are to consider a temporal stability analysis which requires the wavenumber α to be real and a complex frequency $\omega = \omega_R + i\omega_I$. The integration can be performed by means of an adaptive Runge–Kutta method which enables the solution to be resolved accurately in the region of the suspension–clear fluid interface, where rapid variations of the particle concentration arise. At the interface, the matching condition [Eq. (24)] is required to be satisfied but, in view of the fact that only a guess is available for the eigenvalue ω, this condition cannot be met. However, an improvement to ω can be calculated which can then be used as the procedure is repeated, i.e. we shoot from the boundaries to the interface, check whether the matching condition [Eq. (24)] is satisfied and then update ω if necessary. The whole process is continued until we can obtain an eigenvalue which differs from its value at the previous iteration by less than some preassigned tolerance. This method has already been described in more detail in earlier publications, see Shaqfeh and Acrivos (1987) and Zhang et al. (1992).

The base particle concentration and the velocity profiles are given by the solutions of the following equations, see Schaflinger et al. (1990), namely,

$$\int_0^{h_t} \bar{\phi}\bar{U}\,dz = \frac{\phi_s}{1-\phi_s} \tag{25}$$

$$\int_0^{h_t} (1-\bar{\phi})\bar{U}\,dz = 1 \tag{26}$$

$$\frac{d}{dz}\left(\mu_r(\bar{\phi})\frac{d\bar{U}}{dz}\right) = -K \tag{27}$$

and

$$\frac{d\bar{\phi}}{dz} = \frac{-(1-\bar{\phi}) + \kappa K K_c \bar{\phi}}{\kappa \dfrac{d\bar{U}}{dz}\left[(K_\mu - K_c)\dfrac{d\mu_r}{d\phi}\bar{\phi} + K_c\mu_r\right]} \quad \text{for} \quad 0 \le z \le h_t \tag{28}$$

$$= 0 \qquad \text{for} \quad h_t \le z \le 1 \tag{29}$$

subject to the boundary conditions

$$\bar{U} = 0 \quad \text{at} \quad z = 0 \tag{30}$$

and

$$\bar{U} = \bar{\phi} = 0 \quad \text{at} \quad z = 1 \tag{31}$$

5. Numerical results

5.1. Tollmien–Schlichting instabilities for an analytical concentration profile

In order to simplify the problem, and keep the computational time within reasonable bounds, we have opted to neglect the perturbations to the particle concentration. However, one positive aspect provided in this study is that we have been able to consider realistic particle concentration profiles as opposed to the somewhat physically unrealistic piecewise constant profiles which have been considered by several authors, for example, Zhang et al. (1992).

Before introducing our calculated base states, obtained from the solution of the system of Eqs. (25)–(31), we will consider a simpler problem which shows some of the phenomena present in the real situation. In particular, we investigate whether in the region of rapid concentration change, where the particle concentration gradient is subject to a large discontinuity, it is possible to model this by a discontinuity in the concentration itself, as in Yiantsios and Higgins (1988a). We proceed by considering a two-layered flow in which the particle concentration adopts the analytical form

$$\bar{\phi} = 0.4136 \cos\left\{\frac{\pi}{2}(2z)^N\right\} \quad \text{for} \quad 0 \le z \le \frac{1}{2} \tag{32}$$

$$\bar{\phi} = 0 \qquad \text{for} \quad \frac{1}{2} \le z \le 1 \tag{33}$$

where N is a positive integer which is greater than unity, see Fig. 2(a) and (b), which show the variation of the particle concentration and the relative viscosity, respectively, of the suspension across the channel for different values of N. With this analytical form for the concentration, and hence the relative viscosity via the Eq. (7), the base flow velocity is obtained from the solution of Eq. (27) in the regions $0 \le z \le 1/2$ and $1/2 \le z \le 1$ with the no-slip boundary conditions considered at $z = 0$ and 1. Clearly, as $N \to \infty$ the particle concentration in the region $0 \le z \le 1/2$ approaches a uniform profile which corresponds to the viscosity of the suspension in this region being ten times the viscosity of the clear fluid in the region $1/2 \le z \le 1$. The dimensionless pressure gradient, K, see Eq. (27), is taken to be $11/2$ so that the flow is consistent with that considered by Yiantsios and Higgins (1988a). However, it should be noted that the situation of continuity of $\bar{\phi}$, $\mu_r(\bar{\phi})$ and $\bar{U}'$ across $z = 1/2$ is still maintained. For the similar problem considered by Yiantsios and Higgins (1988a), the discontinuity in the concentration and the viscosity at $z = 1/2$ means that the jump conditions, see Yih (1967), have to be satisfied at the interface.

In this test problem the flow stability is considered with respect to a shear mode of the Tollmien–Schlichting type which becomes unstable for large values of the Reynolds number. We follow Yiantsios and Higgins (1988) by taking the relative density between the two layers to be unity, that is $\eta = 0$ in Eq. (7). Our analysis begins with the calculation of the neutral stability curves, i.e. determining where $\omega_I = 0$ for increasing values of N, from which the critical Reynolds numbers, Re_{cr}, were obtained, see Table 1. Since the viscosity in the bottom half of the duct tends to a uniform value as N becomes larger, it could be implied that the value of Re_{cr} will also tend to a particular value. However, from the results presented in Table 1, it is

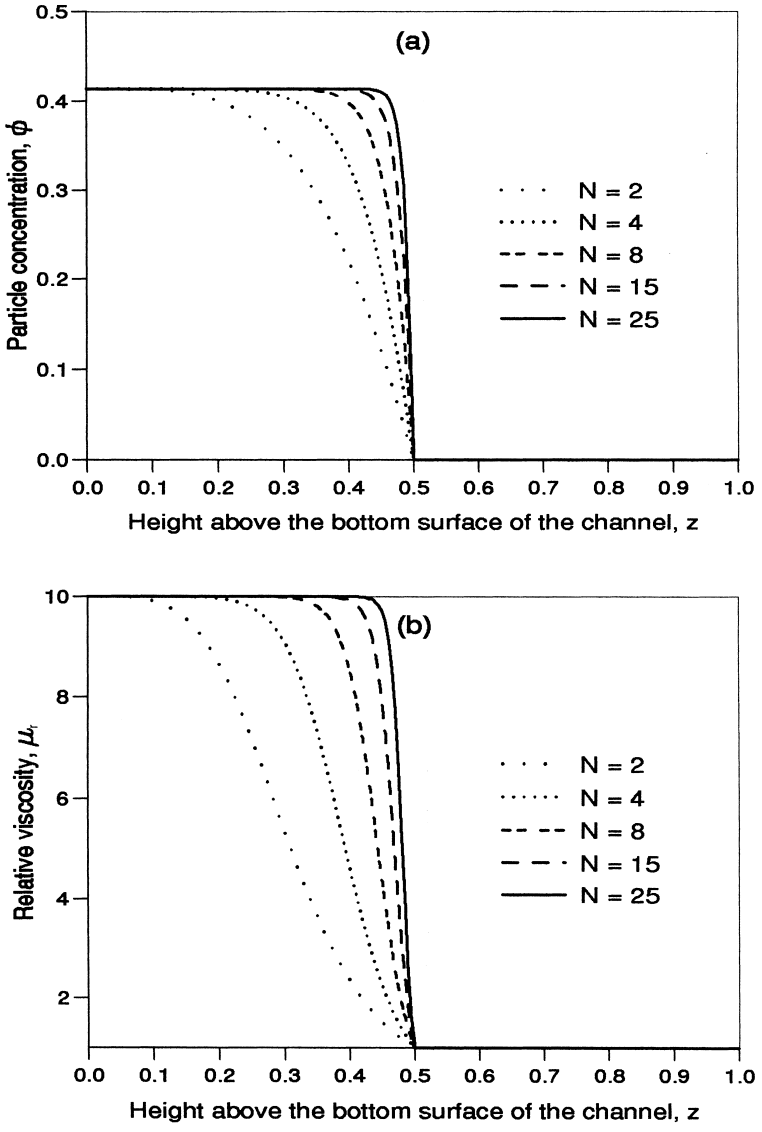

Fig. 2. (a) The variation of the particle concentration, $\bar{\phi}$; and (b) the relative viscosity, $\mu_r(\bar{\phi})$, with the height above the bottom surface of the channel, z.

clear that this is not the case and that Re_{cr} increases as N increases. One might have expected that Re_{cr} would tend to a value close to 20458, which was found by Yiantsios and Higgins (1988a) when there is a jump in the viscosity at $z = 1/2$. In order to investigate why our value for Re_{cr} diverges as N increases it is necessary to examine the modified Orr–Sommerfeld Eq. (22). It becomes apparent that as N increases, the magnitude of the coefficients of the terms in Eq. (22) such as $[(d^2\mu_r)/(dz^2)]$, namely, $= [(d^2\mu_r)/(d\phi^2)]/[(d\phi)/(dz)]^2 + [(d\mu_r)/(dz)]/[(d^2\phi)/(dz^2)]$ become progressively larger in the region of rapid variation of viscosity just below

Table 1
The critical Reynolds numbers, Re_{cr}, for increasing values of N

N	2	3	4	6	8	12	15	20	25
Re_{cr}	7188	11562	16562	24688	31876	51428	70476	108572	169524

the interface $z = 1/2$. As the size of such viscosity gradient coefficients increase, the modified Orr–Sommerfeld Eq. (22) can only be satisfied for the case of neutral stability if Re_{cr} becomes sufficiently large, i.e. of an order comparable to the magnitude of the viscosity gradient coefficients of Eq. (22). Thus, as $N \to \infty$ we require that $Re_{cr} \to \infty$, i.e. the critical value of the Reynolds number for neutral stability continually increases, as the situation in which there is a the discontinuity in the viscosity of the fluid is approached. It should be noted that we were able to replicate the value of Re_{cr}, namely 20458, obtained by Yiantsios and Higgins (1988a) when a jump in viscosity was considered, i.e. when the term involving viscosity gradients was neglected.

The cause of the continual growth in Re_{cr} as $N \to \infty$ is possibly due to the exclusion of the term relating to perturbations in the particle concentration in the full Orr–Sommerfeld Eq. (22). Although the quantity ξ may have a relatively small magnitude, the neglected term, namely, $[1/Re][(d^2)/(dz^2) + \alpha^2]\ [\xi \bar{U}'(d\mu_r)/(d\phi)]$ has an order which is comparable to the terms in Eq. (22) involving viscous gradients. Additionally, the implementation of a fixed suspension–clear fluid interface is physically questionable since in reality the suspension may bulge into the clear fluid or vice versa, however, this is accounted for provided the disturbed interface can be linearized about $z = h_t$.

5.2. Effect of the Reynolds number on the interfacial mode instability

We will now present results which are obtained by solving the base flow system [Eqs. (25)–(31)], together with the modified Orr–Sommerfeld Eq. (22) subject to the boundary conditions [Eq. (23)]. Since the particle concentration within the channel varies continuously, the quantities ψ, ψ', ψ'' and ψ''' are also continuous across the suspension–clear fluid interface. In order to be consistent with Zhang et al. (1992), we take the Galileo number which is given as

$$Ga = \frac{8B^3 g}{\nu_1^2} \tag{34}$$

to be 7.9×10^7, which corresponds to water at 20°C and to a duct spacing $2B = 0.02$ m. The other parameters ϕ_s, η and Re (or κ) were set at various values of practical interest and in particular, Re was allowed to vary up to $O(10^3)$. Within this range of values of Re, any instabilities are due to the interfacial mode as opposed to the Tollmien–Schlichting mode which occurs at large Reynolds numbers, i.e. $Re \sim O(10^4)$. Hence, the remainder of the results will be devoted simply to interfacial mode instabilities and Tollmien–Schlichting instabilities will not be considered further. It should be noted, that the expression for Re in terms of the

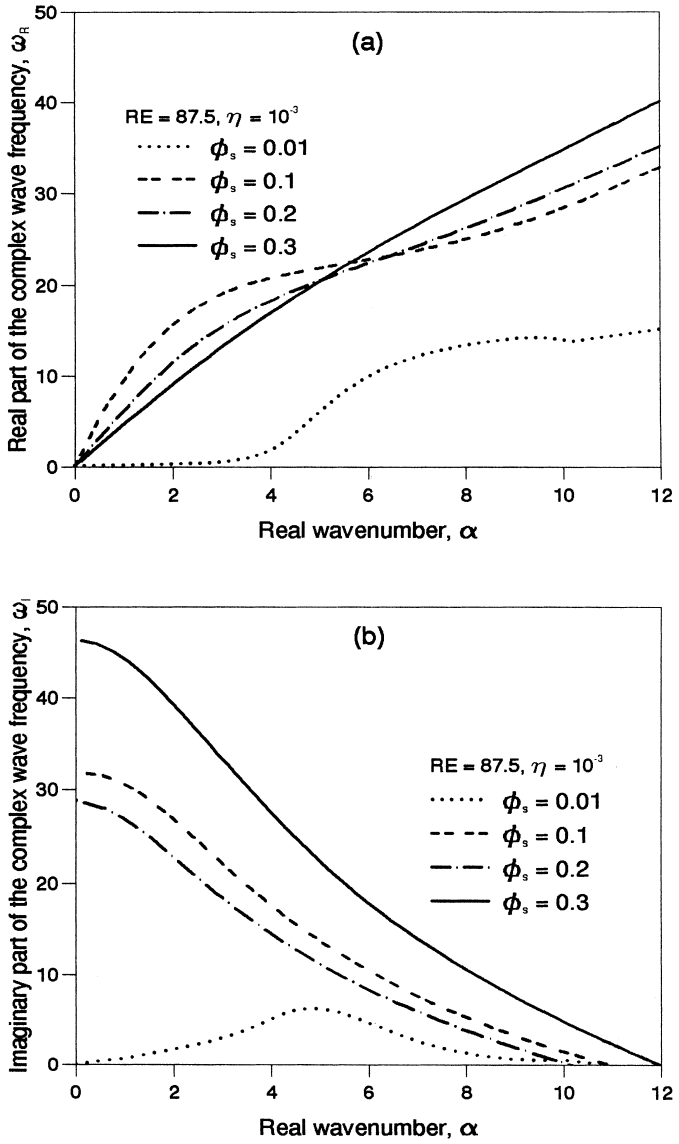

Fig. 3. (a) The variation of the real part, ω_R; and (b) the imaginary part, ω_I, of the complex wave frequency, ω, with the real wavenumber, α, when $Re = 87.5$ and $\eta = 10^{-3}$ for various values of the initial feed particle concentration, ϕ_s.

other parameters that occur in the problem is given by

$$Re = \frac{2}{9}\kappa\eta Ga \tag{35}$$

The instability characteristics of these interfacial disturbances are illustrated in Figs 3–5, where the real and imaginary parts, respectively, of the frequency ω have been plotted against the real

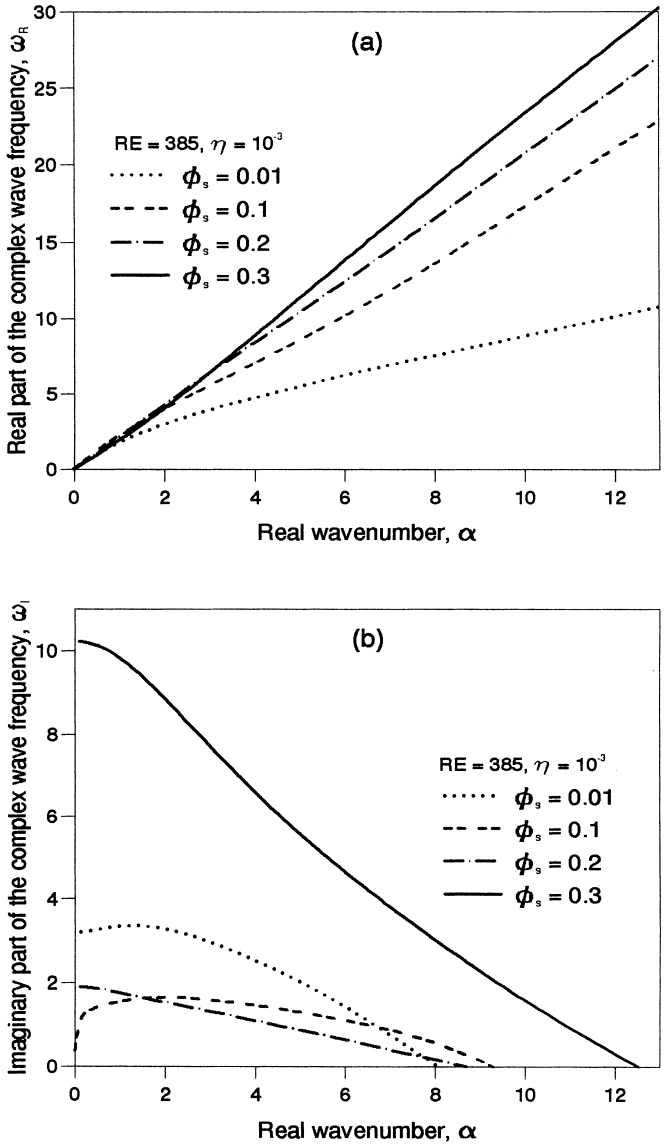

Fig. 4. (a) The variation of the real part, ω_R; and (b) the imaginary part, ω_I, of the complex wave frequency, ω, with the real wavenumber, α, when $Re = 385$ and $\eta = 10^{-3}$ for various values of the initial feed particle concentration, ϕ_s.

wavenumber α for a relative density ratio $\eta = 10^{-3}$, and for a variety of values of the feed concentration ϕ_s and of Re. We choose $\eta = 10^{-3}$ so that stability characteristics can be determined for a variety of different feed concentrations and flow conditions without involving the effects of the stratification of density which are considered separately later. From Fig. 3a, 4a and 5a it can be seen that the real part of the frequency ω_R varies approximately linearly with α, as indicated by Zhang et al. (1992), with the exception of disturbances at large α when

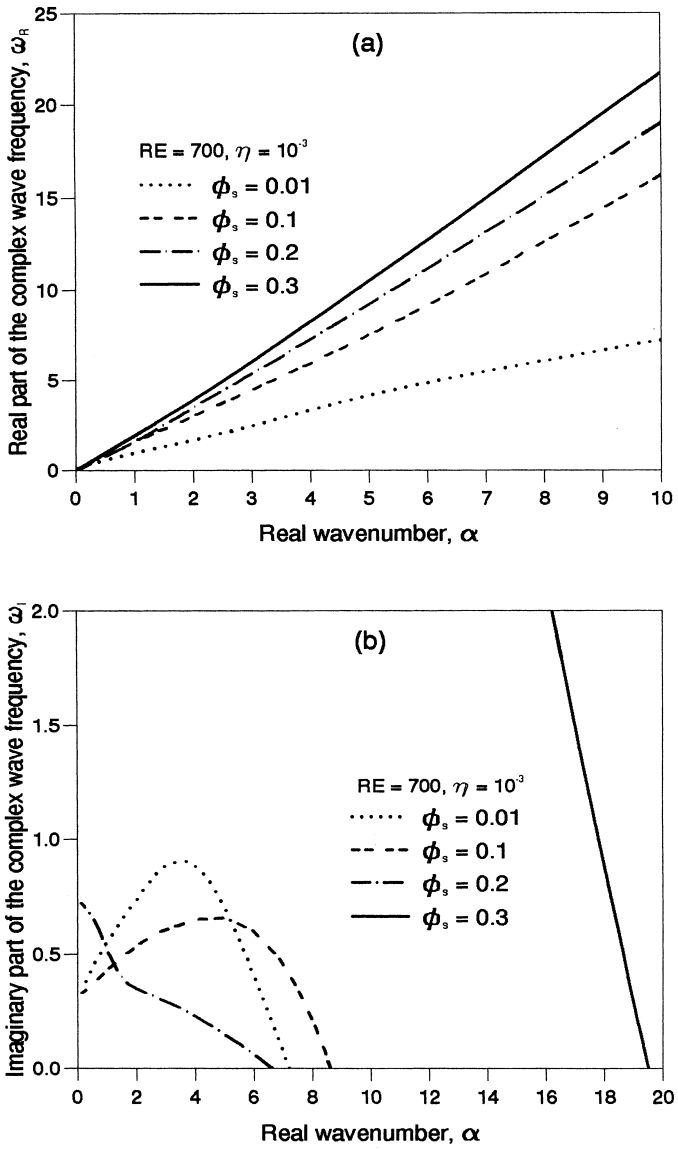

Fig. 5. (a) The variation of the real part, ω_R; and (b) the imaginary part, ω_I, of the complex wave frequency, ω, with the real wavenumber,α, when $Re = 700$ and $\eta = 10^{-3}$ for various values of the initial feed particle concentration, ϕ_s.

$Re = 87.5$. The gradient of ω_R with respect to α represents the group velocity of a wave packet and it can be seen that, at fixed values of Re, these gradients increase with the feed concentration ϕ_s which is in agreement with the results of Zhang et al. (1992). However, it should be noted that when $Re = 87.5$, as shown in Fig. 3a, the gradients of the curves, which represent the group velocity of unstable disturbances, only increase with ϕ_s for values of α greater than ≈ 5. Additionally, from examination of Fig. 3a, 4a and 5a, it is noticeable that the

group velocities of disturbances, at fixed values of ϕ_s, decrease with Re except for the case when $\phi_s = 0.01$. The reason behind such observations is, as yet, unclear and needs further investigation.

It should be noted, see Drazin and Reid (1981), that there is said to be 'convective' instability when no unstable mode exists which has a group velocity equal to zero, because then the disturbance remains small at any fixed point although it grows as it moves downstream. The work of Zhang et al. (1992) established that the disturbances, for the range of parameters they considered, were indeed convective in nature, i.e. the interfacial waves grew as they moved along the channel. We came to a similar conclusion except in the single case when $\phi_s = 0.01$ and the flow Reynolds number is 87.5, see Fig. 3a. In this case it is seen that the gradient of the curve, and hence the group velocity of the disturbance, is very small at small wavenumbers. Hence, in this case there is a possibility that the flow may be 'absolutely' unstable, see Drazin and Reid (1981). In addition, the presence of a local minimum and maximum in the vicinity of $\alpha \simeq 10$ for this particular value of ϕ_s could also suggest the same effect. This occurs if there exists an unstable mode which has a zero group velocity and thus any disturbance will grow at some fixed points. The range of parameters considered in this investigation is by no means exhaustive and thus the existence of other parameter ranges for which absolute instabilities exist cannot be excluded, especially since Schaflinger (1994) showed the presence of such a phenomenon for $\phi_s = 0.0114$ and $Re = 200$.

Fig. 3b, 4b and 5b illustrate how the imaginary part of the frequency ω_I, which determines the growth rates of unstable disturbances, varies with the wavenumber α at values of Re of 87.5, 385 and 700, respectively. It is clear from all these figures that $\omega_I > 0$ for only relatively small values of α, indicating that the flow is susceptible to long wavelength disturbances. In contrast, in the majority of the calculations considered by Zhang et al. (1992) in which a piecewise uniform concentration profile was used $\omega_I > 0$ was found for both small and large values of α. This is illustrated in Fig. 6, which shows the variation of ω_I with α for the piecewise uniform concentration when $Re = 385$ and $\eta = 10^{-3}$. So, for the piecewise uniform base concentration profiles, as considered by Zhang et al. (1992), both long and short wavelength instabilities were found to co-exist for Reynolds numbers up to $O(10^3)$. Whilst this is contrary to the experimental observations of Kao and Park (1972), the phenomena is supported by the work of Schaflinger et al. (1995) who observed the presence of co-existence of both long and short wavelength instabilities, with the long and short wavelengths of the order $40B$ and $2B$, respectively. The assumption made by Zhang et al. (1992) in which uniform concentration and viscosity profiles, with a discontinuity at the interface, are considered is equivalent to ignoring diffusion effects in systems of miscible homogeneous fluids because the diffusion tends to smooth out any discontinuities. In the experiments performed by Tan and Homsy (1988) it was shown that diffusion tends to stabilize short wavelength instabilities. Thus, it could be that the calculations considered by Zhang et al. (1992) have over estimated the influence of short wavelength instabilities, i.e. their effect could be eliminated or reduced if continuous variations in the particle concentration had been considered, however, as the suspension–clear fluid interface remains sharp under most conditions it is likely that the real reason is far more complex.

One possible reason for the predominant effect of long wavelength instabilities when considering continuous base particle concentration profiles can be attributed to the

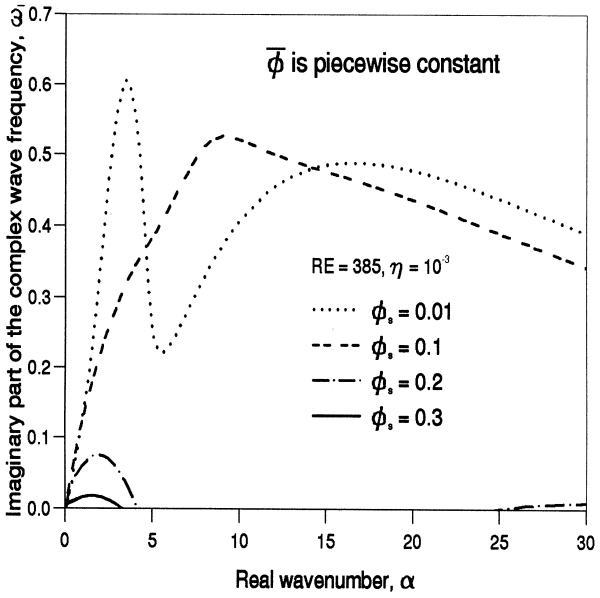

Fig. 6. The variation of the imaginary part, ω_I, of the complex wave frequency, ω, with the real wavenumber, α, with $Re = 385$ and $\eta = 10^{-3}$ for various values of the initial feed particle concentration, ϕ_s when a piecewise constant base particle concentration profile, $\bar{\phi}$, was used.

corresponding base velocity profiles. In particular, the base velocity profile varies smoothly across the whole channel and within any localized region the shear rate appears to be approximately constant, i.e. locally the flow is of a Couette type. It is well known, see Drazin and Reid (1981), that a Couette type flow always becomes unstable as a result of long wavelength disturbances and consequently this is also true for the current case. Alternatively, where a piecewise uniform profile is used as the base state, as in Zhang et al. (1992), the shear rate is discontinuous at the suspension–clear fluid interface and thus the localized flow in this region does not resemble a Couette type flow. Accordingly, for such a flow short wavelength, as well as long wavelength, instabilities abounded. Since 'miscible' fluids usually have an interface across which the viscosity varies smoothly, the former situation, i.e. where the flow is locally of a Couette type, tends to arise very frequently and this may be why long waves always seem to be more predominant. It should be noted that the suspension and the clear fluid are considered as two miscible fluids in the current analysis.

5.3. *Effect of the initial feed concentration on the interfacial mode instability*

In addition, Zhang et al. (1992) showed from their results that the growth rates of the disturbances increase as the initial feed concentration ϕ_s decreases. This enhancement of growth rates was attributed to the fact that the height, h_t, of the suspended layer in the channel decreased dramatically following a decrease in ϕ_s, as required by particle mass conservation in the base flow. It should be recalled that an asymptotic analysis for short wavelength instabilities in the stratified flow of two fluids, see Yiantsios and Higgins (1988a), showed that

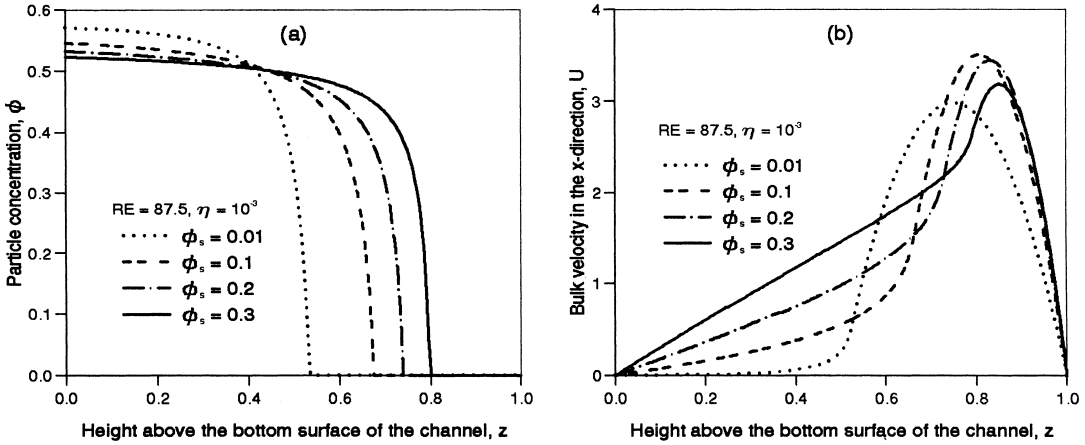

Fig. 7. (a) The variation of the base particle concentration, $\bar{\phi}$; and (b) bulk x-component of velocity $\bar{U}$, with the height above the bottom surface of the channel, z, when $Re = 87.5$ and $\eta = 10^{-3}$ for various values of the initial feed particle concentration, ϕ_s.

the amplification rate ω_I is proportional to the square of the shear rate at the interface; see Hinch (1984) for a simple physical explanation of this instability mechanism. Since the shear rate at the interface is found to be a monotonically decreasing function of h_t, see Schaflinger et al. (1990), the reduction of ϕ_s leads to the pronounced increase in the shear rate and, hence, in the maximum value of ω_I.

This trend, in which the growth rate of disturbances increase as ϕ_s decreases, is not borne out by our results, see Fig. 3b, 4b and 5b, which show that the growth rate is always much larger when $\phi_s = 0.3$ compared with to the other lower values of ϕ_s considered. In particular, apart from the dominant growth that occurs when $\phi_s = 0.3$, there does not seem to be any pattern in the growth rates as ϕ_s decreases at fixed values of Re. Also, the magnitude of the growth rates observed in this study appear to be much larger than those predicted by Zhang et al. (1992) and this may be seen by comparing Fig. 4b and 6, respectively, which refer to the situation when $Re = 385$ and $\eta = 10^{-3}$.

In order to examine our results for the growth rates of disturbances occurring at particular values of ϕ_s in a more critical manner, it is necessary to visualize the base particle concentration and the corresponding velocity profiles associated with each case. Figs. 7a, 8a and 9a depict the particle concentration profiles when Re is 87.5, 385 and 700, respectively, for a variety of values of ϕ_s, while Figs. 7b, 8b and 9b depict the corresponding bulk velocity profiles in the x-direction. From Fig. 7a it can be seen that when $\phi_s = 0.01$ and $Re = 87.5$ the predicted value of the particle concentration in the suspension region is about 0.575. This corresponds to the suspension layer having a relative viscosity of $O(10^4)$ times that of the clear fluid. For values of $\phi_s = 0.1$, 0.2 and 0.3 the corresponding relative viscosity within the suspension layer compared with the clear fluid is only of $O(10^2)$. The very high particle concentration, and hence the very high relative viscosity, of the suspension in the lower region of the channel when $\phi_s = 0.01$ and $Re = 87.5$ ensures that the velocity within this region is vanishingly small. In fact, from Fig. 7b it is noticeable that there is virtually no flow across the

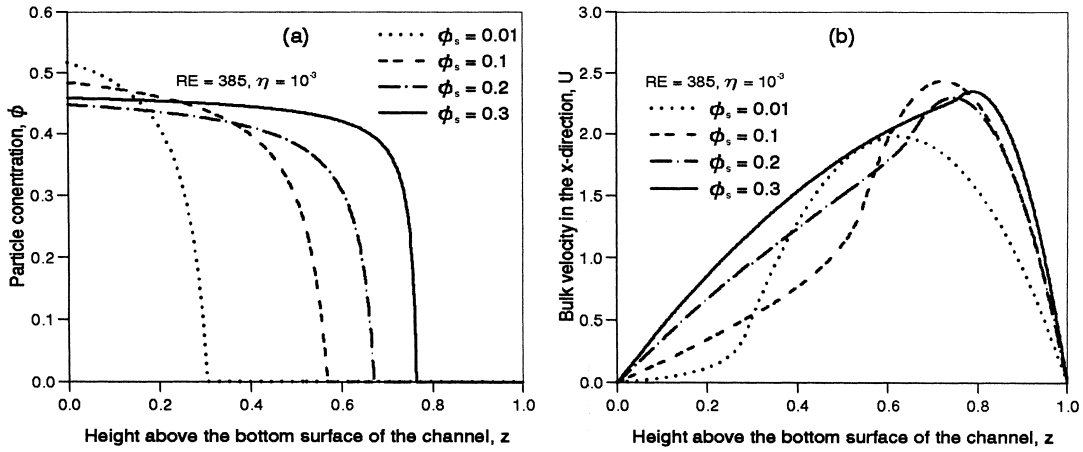

Fig. 8. (a) The variation of the base particle concentration, $\bar{\phi}$; and (b) bulk x-component of velocity $\bar{U}$, with the height above the bottom surface of the channel, z, when $Re = 385$ and $\eta = 10^{-3}$ for various values of the initial feed particle concentration, ϕ_s.

lower half of the channel, which may explain why the growth rate of the disturbances is much smaller when $\phi_s = 0.01$ and $Re = 87.5$ as compared with corresponding values at larger values of ϕ_s. In addition, this may have some bearing on why, as explained earlier, the group velocity of the disturbance occurring when $\phi_s = 0.01$ and $Re = 87.5$, becomes vanishingly small, leading to the possibility of the flow becoming absolutely unstable.

As pointed out earlier, the greatest rate of growth of unstable disturbances, regardless of the value of Re, seems to occur when $\phi_s = 0.3$. One might explain this from an examination of Fig. 7a, 8a and 9a from which it can be observed that the maximum particle concentration,

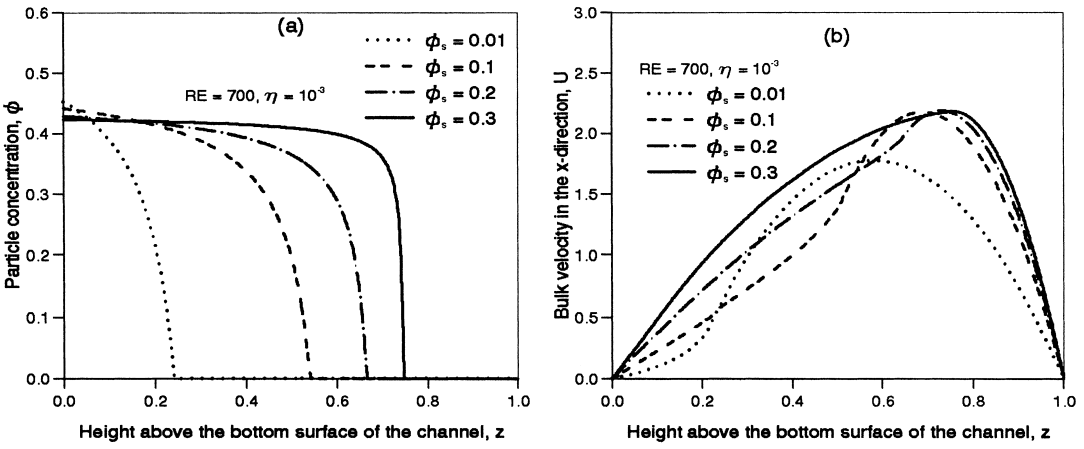

Fig. 9. (a) The variation of the base particle concentration, $\bar{\phi}$; and (b) bulk x-component of velocity $\bar{U}$, with the height above the bottom surface of the channel, z, when $Re = 700$ and $\eta = 10^{-3}$ for various values of the initial feed particle concentration, ϕ_s.

and hence the maximum effective viscosity, within the suspension layer appears to decrease as ϕ_s increases which it would appear might have a destabilizing effect on the flow. Alternatively, from the examination of the bulk velocity profiles for the base states at a variety of values of *Re*, see Fig. 7b, 8b and 9b, it can be seen that its magnitude increases markedly as ϕ_s increases. This is caused by the enhancement of the shear-induced diffusive flux which is due to an increased number of interparticle interactions which have resulted as a direct consequence of increasing ϕ_s. Since inertial effects appear to increase with ϕ_s, the suspension layer may be more susceptible to instabilities at higher values of ϕ_s. However, if this last statement is true, then one can inquire why growth rates of corresponding disturbances, i.e. at the same value of *Re*, occurring when $\phi_s = 0.2$ are smaller in magnitude than those which occur when $\phi_s = 0.1$. This also contradicts the findings of Zhang et al. (1992) who noticed that the growth rates of long wavelength instabilities, as well as short wavelength instabilities, diminished in magnitude as ϕ_s increased.

In order to address these discrepancies it is necessary to refer back to the beginning of this section. In particular, it should be recalled that a continuous artificial base particle concentration profile was introduced in order to approximate the situation in which the relative viscosity of the suspension changed discontinuously at the interface with the clear fluid. The profile was constructed so that by simply increasing the value of an adjustable parameter, *N*, the concentration was able to approach the discontinuous situation. From these calculations it was found that the neutral stability curve for our flow did not resemble the known neutral stability curve for the discontinuous profile even as the continuous profile approached such a profile. Instead the critical value of *Re*, beyond which the flow became unstable, was found to diverge as the continuous concentration profile became steeper in the vicinity of the interface in order to approximate the discontinuity. It was concluded that the increasingly large gradients in the particle concentration and the effective viscosity encountered as the discontinuity was approached, and the absence of terms with similar orders of magnitude involving perturbations to the particle concentration, lead to a blow up of viscous gradient terms in the governing modified Orr–Sommerfeld Eq. (22) and hence gave rise to spurious results. Such an occurrence may possibly give an explanation for the uncharacteristic behaviour of the growth rates of the instabilities considered in the current analysis.

In order to analyse such a claim we present Figs 10–12 which illustrate how the gradients of the base particle concentration profiles vary across the channel when $Re = 87.5$, 385 and 700, respectively. From these figures the most striking observation is that the magnitude of the gradient in the particle concentration, at a fixed value of *Re*, is always the largest at the suspension–clear fluid interface when $\phi_s = 0.3$. In fact, the difference in the magnitude of the maximum gradients in the particle concentration at other values of ϕ_s compared to those when $\phi_s = 0.3$ is always very substantial. The size of such gradients when $\phi_s = 0.3$ suggest that the coefficient $(d^2\mu_r)/(dz^2)$ has an order of magnitude of at least 10^4 and in the case when $Re = 700$, which is illustrated in Fig. 12, the value of $(d^2\mu_r)/(dz^2)$ has a magnitude of about 10^5, i.e. the terms involving the coefficient $(d^2\mu_r)/(dz^2)$ are likely to swamp the other terms within the modified Orr–Sommerfeld Eq. (22), as described earlier, and consequently the solutions of this equation will be dramatically altered. From these findings it appears that the results obtained when $\phi_s = 0.3$, irrespective of the value of *Re*, may all be spurious in nature and thus cannot be relied upon. However, by initially re-analysing the results presented in

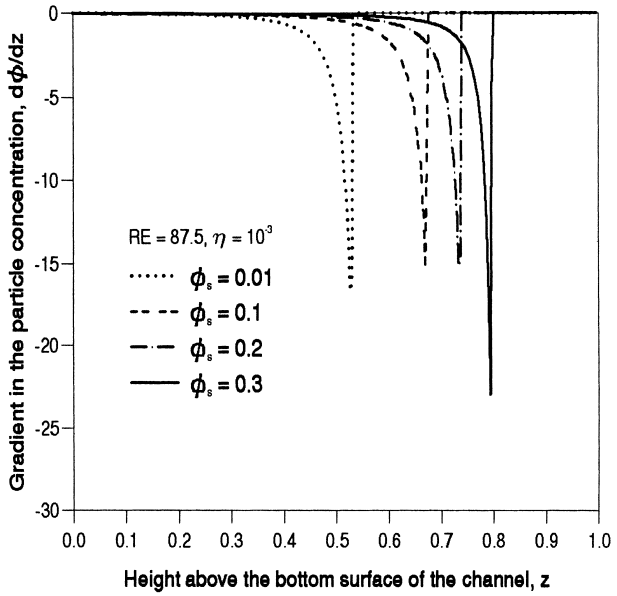

Fig. 10. The variation of the gradient in the base particle concentration, $(d\bar{\phi})/(dz)$, with the height above the bottom surface of the channel, z, when $Re = 87.5$ and $\eta = 10^{-3}$ for various values of the initial feed particle concentration, ϕ_s.

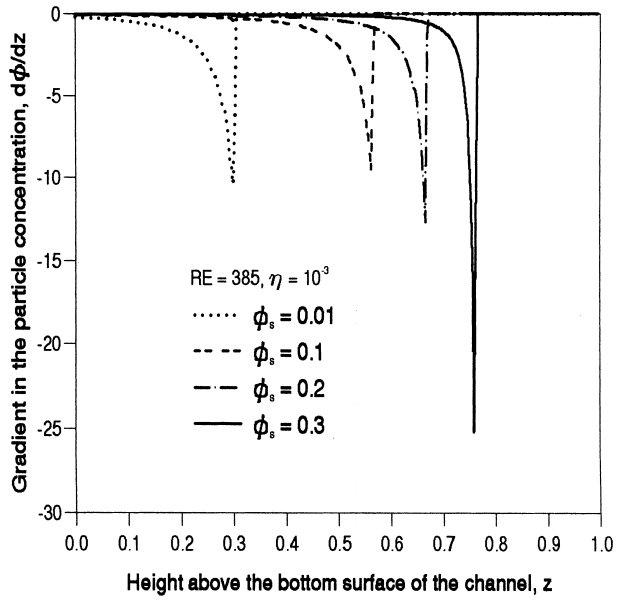

Fig. 11. The variation of the gradient in the base particle concentration, $(d\bar{\phi})/(dz)$, with the height above the bottom surface of the channel, z, when $Re = 385$ and $\eta = 10^{-3}$ for various values of the initial feed particle concentration, ϕ_s.

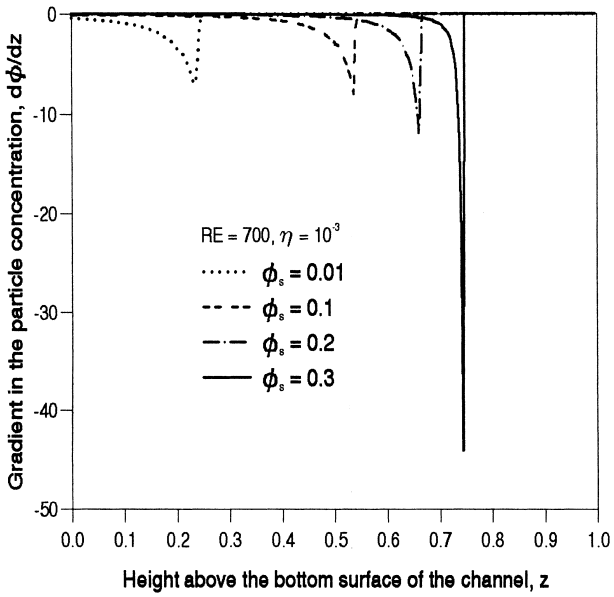

Fig. 12. The variation of the gradient in the base particle concentration, $(d\bar{\phi})/(dz)$, with the height above the bottom surface of the channel, z, when $Re = 700$ and $\eta = 10^{-3}$ for various values of the initial feed particle concentration, ϕ_s.

Fig. 4b and 5b, which show the growth rates of unstable disturbances for a variety of values of ϕ_s when $Re = 385$ and 700, respectively, it can be seen that apart from the results presented at very small wavenumbers the growth rates of the instabilities appear to increase in magnitude as ϕ_s decreases. Hence, although the results may not be quantitatively sound, at least they appear to be in qualitative agreement with the work of Zhang et al. (1992). This result seems to be intuitively correct since as ϕ_s increases so does the height of the suspension layer, as indicated in Fig. 7a, 8a and 9a, resulting in an increase in the effective viscosity across a larger region of the channel which thus has a stabilizing effect on the flow.

Now by returning to Fig. 3b, which shows the growth rates of unstable disturbances for a variety of values of ϕ_s when $Re = 87.5$, it is plain that the growth rates, even after the exclusion of the result when $\phi_s = 0.3$, are very large and do not follow the qualitative behaviour expected. On examination of Fig. 10 it can be seen that the gradient in the particle concentration has a magnitude of at least 15 compared with about 10 or less for the corresponding cases when $Re = 385$ and 700. Thus, when $Re = 87.5$, the large magnitude of the viscosity gradient coefficients such as $(d^2\mu_r)/(dz^2)$ may once again affect the validity of the modified Orr–Sommerfeld Eq. (22) and put the results obtained for this case into doubt. However, it should be stressed that even with the questionable nature of some of these results the approach adopted is still a move in the right direction with an attempt to introduce the physically observed particle concentration profile with its rapidly changing concentration value close to the interface, as opposed to the more artificial discontinuous concentration model. Since such a model clearly highlights the cause of why some of the results may be dubious and how with enhanced computer power the matter could be resolved. In addition, it makes the

stability analysis of the discontinuous concentration model presented by Yiantsios and Higgins (1988a) questionable, since such results cannot be approached from the continuous model utilizing Eqs. (32) and (33) as N increases.

By referring to Fig. 4b and 5b one can see a trend indicating a decrease in the maximum magnitude of the growth rates of the unstable disturbances at a particular value of ϕ_s, as Re increases from 385 to 700. In fact, as Re increases from 385 to 700, the maximum growth rates of the unstable disturbances all decrease by at least a factor of three. It should be recalled that such a trend was also observed by Zhang et al. (1992). This trend is further illustrated by Fig. 13 which shows the variations of ω_I with α for various values of ϕ_s when $Re = 1000$ and $\eta = 10^{-3}$. In particular, the magnitude of the growth rates decrease as Re increases from 700 to 1000. Additionally, the results again agree with the findings of Zhang et al. (1992) since the magnitude of the growth rates when $Re = 1000$ decrease with increasing ϕ_s. This result is true except at very small values of α when $\phi_s = 0.2$. The reason for this may be due to the presence of increasing magnitudes of the particle concentration gradients as Re increases which is the reason why results for $\phi_s = 0.3$ have not been presented in this case. From such results it may be possible to infer that instabilities due to the interfacial mode restabilize at a sufficiently large value of Re, provided that the magnitudes of particle concentration gradients remain reasonably small in the region of the suspension–clear fluid interface. Nevertheless, it should be

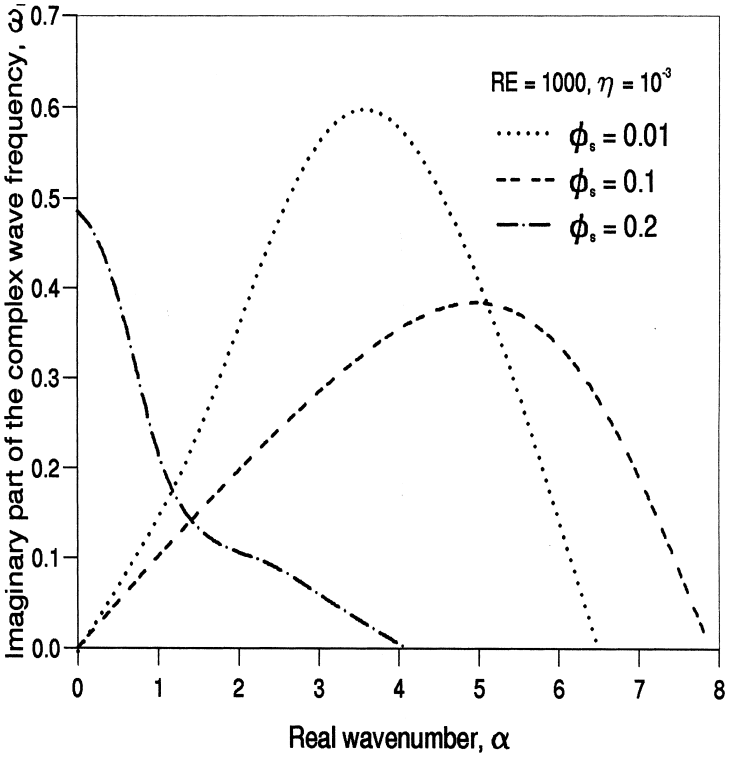

Fig. 13. The variation of the imaginary part, ω_I, of the complex wave frequency, ω, with the real wavenumber, α, when $Re = 1000$ and $\eta = 10^{-3}$ for various values of the initial feed particle concentration, ϕ_s.

emphasized that this does not imply the existence of an experimentally observable restabilization of unstable interfacial waves in such flows, because on account of three-dimensional disturbances an increase in the values of *Re* does not restabilize the flow, but rather changes the direction of the growing modes and, more specifically, that of the most rapidly amplified mode which in general is oblique when compared with other growing modes, see Magen and Patera (1986). In any case, it is very probable that an unstable mode of the Tollmien–Schlichting type will manifest itself well before the present unstable disturbance appears to become stable.

Apart from reducing the magnitude of the growth of the unstable modes, it can also be seen that the range of values of α for which the flow is unstable tends to decrease as *Re* increases. This is further illustrated on examination of Fig. 14, which depicts the neutral stability curves for flows in which $\phi_s = 0.1$ and 0.3, where $\eta = 10^{-3}$. In particular, when $\phi_s = 0.1$ it is clear that the range of values of α for which instabilities occur decreases with an increase in *Re*. This is an obvious consequence of the diminishing growth rates which were discussed above, i.e. for certain values of α an overall reduction in the growth rate will mean that unstable disturbances will appear to restabilize as *Re* increases and hence it will appear that the range of values of α for which instabilities exist is reduced. When $\phi_s = 0.3$ it can be seen that the range of α for which instabilities exist increases rapidly for *Re* greater than about 300. Again, the most likely cause is that when $\phi_s = 0.3$ the limit of total resuspension is approached at much lower values

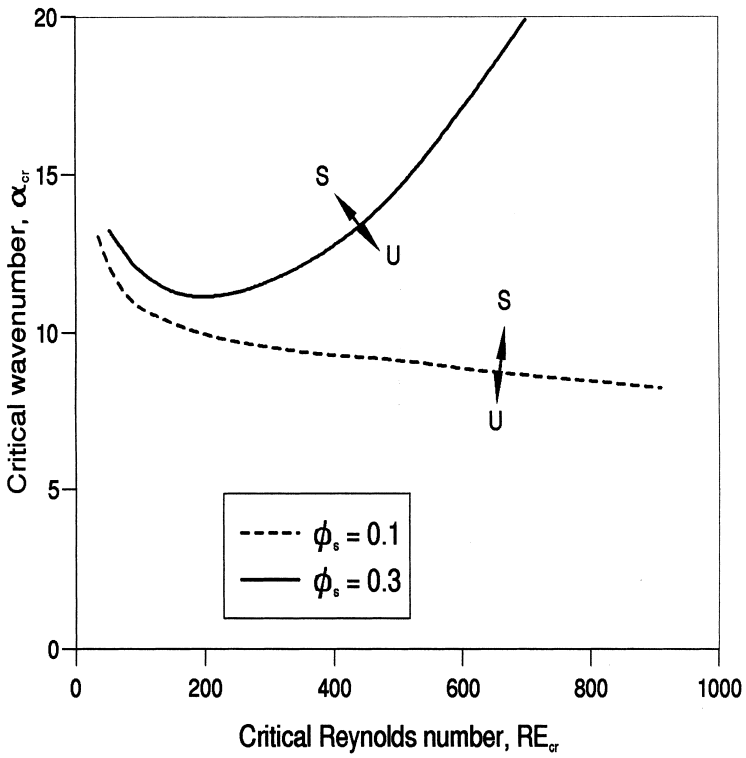

Fig. 14. The neutral stability diagram for $\eta = 10^{-3}$ when the initial feed particle concentration, ϕ_s, is 0.1 and 0.3.

of Re than it would be for lower values of ϕ_s, i.e. when $\phi_s = 0.3$ there are many more interparticle interactions occurring than would be the situation at lower values of ϕ_s, thus leading to a greater amount of migration of particles. Consequently, discontinuous particle concentration and relative viscosity profiles are being approached which gives rise to the rapid increase in the magnitude of the eigenvalues, as discussed earlier in this section.

It should be noted that the neutral stability diagram, shown in Fig. 14, representing our calculations is quite different qualitatively to the corresponding diagram produced by Zhang et al. (1992). In our case, irrespective of the value of Re, instabilities always take the form of long wavelength disturbances. However, Zhang et al. (1992) found that at a particular value of Re the wavelengths of the unstable disturbances are within two distinct ranges, long and short, respectively, and with increasing Re disturbances over the whole spectrum of wavelengths become unstable. However, by ignoring the instabilities associated with short wavelength disturbances, whose effect is most certainly over estimated, the discrepancy between the current work and the neutral stability curves of Zhang et al. (1992) is reduced. In principle, we would have qualitative agreement in such a situation except within the region in which $Re < 10^2$, since here the validity of our analysis is uncertain, as discussed earlier.

5.4. Interfacial mode instabilities for an analytical concentration profile

The results considered at the beginning of this section involved the utilization of a continuously varying artificial particle concentration profile in which the magnitude of the discontinuity of the gradient continued to increase. However, all the calculations performed were exclusively in the range where the Reynolds number was large, corresponding to the instability mode of the Tollmien–Schlichting type. Naturally, for completeness, it would be useful to analyse the behaviour of instabilities which occur at small values of Re, i.e. those due to the interfacial mode. In particular, the situation is considered in which an artificial concentration profile approaches the discontinuous gradient case used to obtain the results illustrated in Fig. 6, namely, when $\phi_s = 0.1$, $Re = 385$ and $\eta = 10^{-3}$, with $\bar{\phi} = 0.41$ and $h_t = 0.56$. Therefore, a continuous function for which the magnitude of the discontinuity in the gradient as N becomes large approaches that in the concentration, is given by

$$\bar{\phi} = 0.41 \cos\left\{\frac{\pi}{2}\left(\frac{z}{0.56}\right)^N\right\} \quad \text{for} \quad 0 \le z \le 0.56 \tag{36}$$

$$= 0 \qquad \text{for} \quad 0.56 \le z \le 1 \tag{37}$$

where N is a positive integer greater than unity, see Fig. 15 which shows the variation of the particle concentration across the channel for different values of N. The maximum value of $\bar{\phi}$ has to be set at 0.41 compared with a value of 0.47 in order that the mean concentration of the model as $N \to \infty$ agrees with that from the concentration profile in Fig. 8a. Fig. 16 shows how ω_I varies with α for different values of N and how it compares to the discontinuous solution. It is clearly seen that as N increases from 8 to 16 the behaviour of the unstable mode deviates significantly from the mode corresponding to the discontinuous situation, i.e. the maximum magnitude of the growing mode increases five fold as N increases from 8 to 16 and it diverges

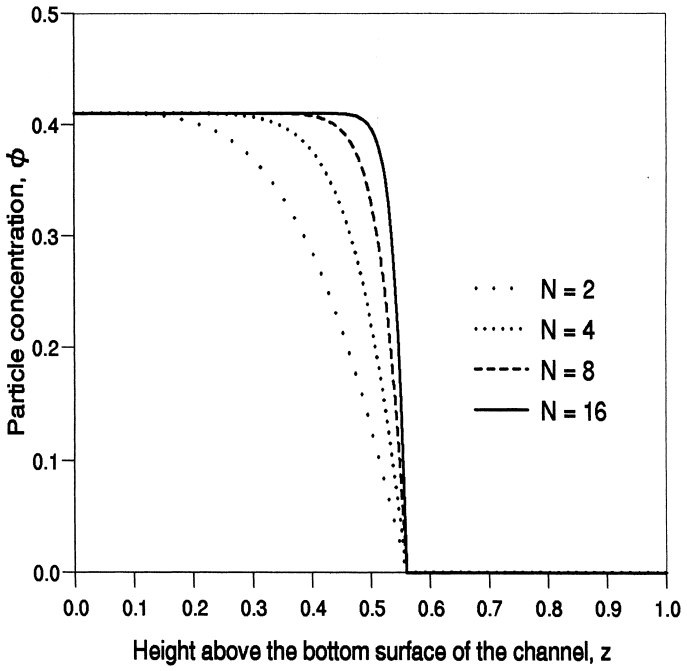

Fig. 15. The variation of an analytical particle concentration, $\bar{\phi}$, with the height above the bottom surface of the channel, z, for increasing values of N.

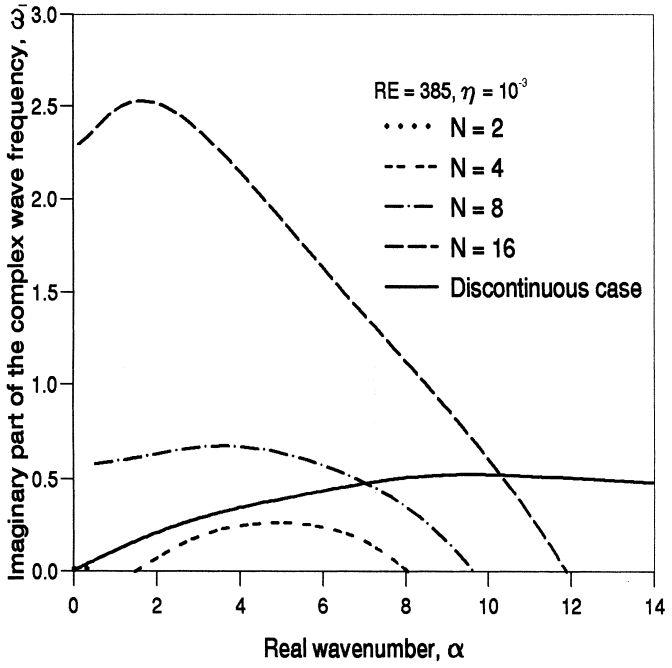

Fig. 16. The variation of the imaginary part, ω_I, of the complex wave frequency, ω, with the real wavenumber, α, when $Re = 385$ and $\eta = 10^{-3}$ for a analytical base particle concentration profile, $\bar{\phi}$, with increasing values of N.

from the growing mode obtained by using the constant particle concentration profile with a discontinuity at the interface. This type of behaviour has all the typical hallmarks which were associated with the results obtained when $\phi_s = 0.3$. However, this discrepancy between the results from the limiting situation and those from the limit itself should not cause undue concern since it arises solely due to the mathematical model being solved. If one is to recover the limit situation from the limiting situation then the Orr–Somerfeld representation of the instabilities in the limiting situation must be such that it nullifies the strong concentration gradients in the suspension close to the suspension–clear fluid interface from radically changing its solution. At present exactly how this modification to the equation should be undertaken is unclear, and whether the extra contributions from the neglected concentration perturbations would rectify the model is debatable, but the fact remains that the introduction of a more physical representation of the basic flow is distorting the governing linear stability model from the form this equation would assume at its limit.

5.5. *Effect of density stratification on the interfacial mode instability*

As mentioned in Section 5.2, we now examine what effect density stratification has on the stability of the flow. Fig. 4b and Fig. 17 show how the imaginary part of the frequency ω_I varies with the wavenumber α when $\eta = 10^{-3}$ and $\eta = 0.1$, respectively, for various values of ϕ_s when $Re = 385$. It should be noted that by changing the value of η we need to modify either κ or Ga if the value of the flow Reynolds number, Re, is to remain unchanged, see

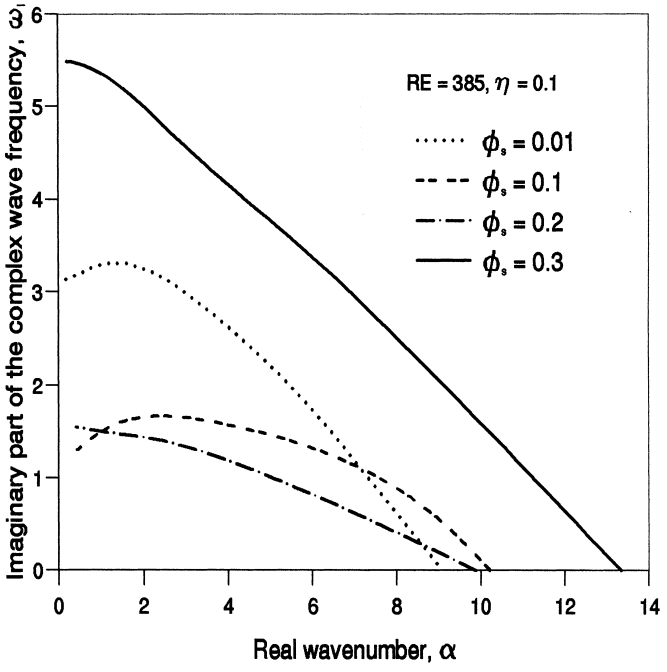

Fig. 17. The variation of the imaginary part, ω_I, of the complex wave frequency, ω, with the real wavenumber, α, when $Re = 385$ and $\eta = 10^{-1}$ for various values of the initial feed particle concentration, ϕ_s.

Eq. (35). Unfortunately, by changing κ, the base particle concentration and bulk velocity profiles will be altered and so it would be difficult to make a comparison between the calculation performed at $\eta = 10^{-3}$ and 0.1. By decreasing Ga from 7.9×10^7 to 7.9×10^5, whilst increasing η from 10^{-3} to 0.1, we are able to impose Re at 385 without changing κ, which is set as 2.2×10^{-2}. Further, because the governing base flow Eqs. (25)–(31), together with the modified Orr–Sommerfeld Eq. (22) and its corresponding boundary conditions [(Eq. (23)], are independent of Ga the stability of the flow is only influenced by the variation of η. However, by changing Ga we are effectively altering either the height of the channel or the viscosity of the clear fluid, which would be very inconvenient if an experiment was to be contemplated. In any case, on comparison of the figures it can be seen that an increase in density stratification has a stabilizing effect in that the magnitude of the interfacial growing modes diminish regardless of the value of ϕ_s. This observation is in agreement with what has been found by other researchers including Yih (1967) and Yiantsios and Higgins (1988a,b). It should be noted that this result relates to the situation where the density stratification alone is enhanced. If η was increased and κ was decreased while Re and Ga were kept constant, the stability of he flow would be affected by a combination of two effects, namely, the enhancement of viscous stratification which is the driving force for the instability, and the stabilizing effect of greater density stratification. The work of Zhang et al. (1992) has focussed on such complex matters, however, since their results are rather more involved than ours a direct comparison is very difficult.

6. Conclusions

In this paper a linear stability analysis has been presented dealing with the formation of interfacial waves in a two-dimensional Hagen–Poiseuille resuspension flow. The base particle concentration and bulk velocity of the suspension were calculated from the solution of the laminar resuspension flow problem considered by Schaflinger et al. (1990). The nonlinear nature of the particle concentration within the suspension layer was included in our analysis, however, the effects of fluctuations in the particle concentration were ignored because of the numerical difficulties their inclusion would cause.

Numerical solutions of the resulting modified Orr–Sommerfeld system of equations were then obtained by means of a classical shooting method with the aid of orthonormalization. The computations initially focussed on the instabilities due to the Tollmien–Schlichting mode which resulted at Reynolds numbers of $O(10^4)$. In these calculations a continuously varying artificial base particle concentration was employed, from which the corresponding base velocity profile could be obtained, which could be adjusted by means of a parameter to approach a discontinuous piecewise constant particle concentration profile. It was found that as the magnitude of the discontinuity in the gradient of the continuous profile continued to increase the critical Reynolds number at which the flow became unstable increased without any upper bound instead of converging to a known value. Consequently, it was shown that the terms involving coefficients of viscosity gradients within the modified Orr–Sommerfeld equation grew rapidly as the discontinuous situation was approached. It was concluded that such behaviour might have resulted from the fact that we neglected terms involving fluctuations in the particle

concentration even though in certain situations they have an order of magnitude comparable to the terms involving viscosity gradients.

Computations were then considered which dealt with instabilities due to the interfacial mode which occurred at Reynolds numbers of O(1) and above. In this case the base particle concentration and velocity profiles were calculated from the governing momentum, particle diffusion and conservation of mass equations. The validity of the solutions obtained were again brought into question especially in situations where the magnitude of the base particle concentration profile was large in the vicinity of the suspension–clear fluid interface. Consequently, the solutions obtained in such situations were ignored since they were considered to be spurious in nature.

The results of our computations predict that interfacial instabilities are always a result of long wavelength disturbances. It was also found that the resuspension flow was convectively unstable, i.e. disturbances grew as they were convected downstream. However, the state of absolute instability, where disturbances grow at fixed points in space, was possible when the feed concentration was very small. The possible existence of this latter class of instability for a different parameter range cannot be excluded. The group velocity of the unstable disturbances tended to be almost linear in nature and their magnitude appeared to increase with increasing feed concentration and decrease with an increase in the flow Reynolds number. The rate of growth of unstable disturbances was found to increase when the initial feed concentration was decreased and vice versa. In addition, it was predicted that both the growth rates of instabilities and the range of wavenumbers for which they occur decrease as the flow Reynolds number increases. This apparent restabilization of the resuspension flow was discounted since there is evidence that the largest growing modes usually changes its direction of growth as the flow Reynolds number increases. Finally, it was shown that an increase in the density stratification of the flow has a stabilizing effect.

The principal assumption made to simplify computations, i.e. the neglect of fluctuations in the particle concentration, has limited the validity of the linear stability analysis performed. In particular, any resuspension flow in which a steep particle concentration profile exists, be it in a situation where total resuspension is being approached or where a stagnant sediment layer exists, may lead to the production of spurious results. Such problems may only be resolved if the fluctuations in the particle concentration are included which will require an increase in the CPU used for the already difficult calculations. However, the calculations are a considerable step in the right direction in that a continuous concentration profile has been utilized, as compared with that of the more unrealistic piecewise constant profile utilized by Zhang et al. (1992).

References

Acrivos, A., Herbolzheimer, E., 1979. Enhanced sedimentation in settling tanks with inclined walls. J. Fluid Mech. 92, 435–457.

Borhan, A., 1989. An experimental study of the stability and efficiency of inclined supersettlers. Phys. Fluids A 1, 108–124.

Borhan, A., Acrivos, A., 1988. The sedimentation of nondilute suspensions in inclined settlers. Phys. Fluids 31, 3488–3501.

Conte, S.D., 1966. The numerical solution of linear boundary value problems. SIAM Rev. 8, 309–321.
Davis, R.H., Herbolzheimer, E., Acrivos, A., 1983. Wave formation and growth during sedimentation in narrow tilted channels. Phys. Fluids 26, 2055–2064.
Drazin, P.G., Reid, W.H., 1981. Hydrodynamic Stability. Cambridge University Press, Cambridge.
Herbolzheimer, E., 1983. Stability of the flow during sedimentation in inclined channels. Phys. Fluids 26, 2043–2054.
Hinch, E.J., 1984. A note on the mechanism of the instability of the interface between two shearing fluids. J. Fluid Mech. 144, 463–465.
Hooper, A.P., Boyd, W.G.C., 1983. Shear-flow instability at the interface between two shearing fluids. J. Fluid Mech. 128, 507–528.
Hooper, A.P., Boyd, W.G.C., 1987. Shear-flow instability due to a wall and a viscous discontinuity at the interface. J. Fluid Mech. 179, 201–225.
Joseph, D.D., Renardy, Y.Y., 1993. Fundementals of two-fluid dynamics. Springer, New York.
Kao, T.W., Park, C., 1972. Experimental investigations of the stability of channel flows. Part 2. Two-layered co-current flow in a rectangular channel. J. Fluid Mech. 52, 401–423.
Kapoor, B., Acrivos, A., 1995. Sedimentation and sediment flow in settling tanks with inclined walls. J. Fluid Mech. 290, 39–66.
Kojima, M., Hinch, E.J., Acrivos, A., 1984. The formation and expansion of a toroidal drop moving in a viscous fluid. Phys. Fluids 27, 19–32.
Korteweg, D., 1901. Sur la forme que prennent les equations du mouvement des fluids si l'on tient compte des forces capillaires cause par des variations de densite. Arch. Neerl. Sci. Exactes et Naturelles Series 11, 6.1..
Leighton, D., Acrivos, A., 1986. Viscous Resuspension. Chem. Engng Sci. 41, 1377–1384.
Magen, M., Patera, A.T., 1986. Three-dimensional linear instability of parallel shear flows. Phys. Fluids 29, 364–367.
Miskin, I., Elliott, L., Ingham, D.B., Hammond, P.S., 1996a. Viscous resuspension of particles in an inclined rectangular fracture. Int. J. Multiphase Flow 22, 403–415.
Miskin, I., Elliott, L., Ingham, D.B., Hammond, P.S., 1996b. Steady suspension flows into two-dimensional horizontal and inclined channels. Int. J. Multiphase Flow 22, 1223–1246.
Phillips, R.J., Armstrong, A.R., Brown, R.A., Graham, A.L., Abbott, J.R., 1992. A constitutive equation for concentrated suspensions that accounts for shear-induced particle migration. Phys. Fluids A 4, 30–40.
Schaflinger, U., 1994. Interfacial instabilities in a stratified flow of two superposed fluids. Fluid Dynamics Res. 13, 299–316.
Schaflinger, U., Acrivos, A., Zhang, K., 1990. Viscous resuspension of a sediment within a laminar and stratified flow. Int. J. Multiphase Flow 16, 567–578.
Schaflinger, U., Acrivos, A., Stibi, H., 1995. An experimental study of viscous resuspension in a pressure-driven plane channel flow. Int. J. Multiphase Flow 22, 693–704.
Schneider, W., 1982. Kinematic-wave theory of sedimentation beneath inclined walls. J. Fluid Mech. 120, 323–346.
Shaqfeh, E.S.G., Acrivos, A., 1987. The effects of inertia on the stability of the convective flow in inclined settlers. Phys. Fluids 30, 960–973.
Tan, C.T., Homsy, G.M., 1988. Stability of miscible displacements in porous media: rectilinear flow. Phys. Fluids 29, 3549–3556.
Yiantsios, S.G., Higgins, B.G., 1988a. Numerical solution of eigenvalue problems using the compound matrix method. J. Comp. Phys. 74, 25–40.
Yiantsios, S.G., Higgins, B.G., 1988b. Linear stability of plane Poiseuille flow of two superposed fluids. Phys. Fluids 31, 3225–3238.
Yih, C.S., 1967. Instability due to viscous stratification. J. Fluid Mech. 27, 337–352.
Yu HS, Sparrow, E.M., 1969. Experiments on two-component stratified flow in a horizontal duct. Trans. ASME 91, 51–58.
Zhang, K., Acrivos, A., 1994. Viscous resuspension in fully developed laminar pipe flows. Int. J. Multiphase Flow 20, 579–591.
Zhang, K., Acrivos, A., Schaflinger, U., 1992. Stability in a two-dimensional Hagen–Poiseuille resuspension flow. Int. J. Multiphase Flow 18, 51–63.